Dielectric Normal and Segmental Modes in Undiluted Poly(butylene oxide)

Minoru Yamane, Yuji Hirose,† and Keiichiro Adachi*

Department of Macromolecular Science, Graduate School of Science, Osaka University, Toyonaka, Osaka 560-0043, Japan

Received July 25, 2005; Revised Manuscript Received August 19, 2005

ABSTRACT: Dielectric measurements were carried out on undiluted poly(butylene oxide) (PBO) with various molecular weights. The dielectric normal mode relaxation due to fluctuation of the end-to-end vector and the segmental relaxation due to local motions were observed. The relaxation time τ_n for the normal mode and τ_s for the segmental mode conformed to the Vogel−Fulcher equation, and the ratio of τ_n/τ_s did not depend on temperature. From the relaxation strengths for the normal and segmental modes, the parallel and perpendicular components of the dipole moment were determined. With the aid of the literature data of the end-to end distance, the dipole moment per unit contour length of PBO chains was also determined. It was found that the M dependence of τ_n changed around the characteristic molecular weight M_c (=6000), i.e., in the range of $M < M_c$, τ_n is proportional to $M^{2.0}$, and in the range $M > M_c$ τ_n is proportional to $M^{3.4}$. The relationship between the segmental dynamics and chain dynamics is discussed.

Introduction

Polyethers having a chemical structure of $-(CH_2-CHR-O-)_n$ are a typical group of type A polymers which have the dipole moments aligned in parallel with the chain contour and exhibit dielectric normal mode relaxation.[1−3] Baur and Stockmayer first reported the dielectric normal mode relaxation of poly(propylene oxide) (PPO, R = CH_3) in 1965.[4,5] In the 1990s several authors reinvestigated the dielectric behavior of PPO.[6−8] However, those data are limited to the behavior of low molecular weight (MW) samples obeying the Rouse theory.[9] Recently, Kyritsis et al. reported the dielectric normal mode relaxation of poly(butylene oxide) (PBO) with R = $-CH_2CH_3$ and block copolymer composed of PBO and poly(ethylene oxide).[10,11] They also used very low MW PBO. So far the normal mode relaxation covering a wide range of MW has been reported only for two polymers, namely *cis*-polyisoprene (*cis*-PI)[12−16] and poly(lactic acid) (PLA).[17] Although the dielectric normal mode relaxation has been investigated extensively for *cis*-polyisoprene(PI),[3,12−16,18−26] the dielectric data of type A polymers other than PI are needed for studies of chain dynamics in various complex systems such as polymer blends in which the miscibility depends on the chemical structures of the components. Such data are also needed to understand the relationship between the global chain dynamics and local segmental dynamics in which the latter depends strongly on the chemical structure of the repeat units. This paper reports the dielectric relaxation of PBO over a wide range of MW.

Through the dielectric normal mode spectroscopy, one can obtain information on the chain dimension as well as the chain dynamics.[1−3] If the dipole moment per unit contour length is known, the mean-square end-to-end distance can be determined from the relaxation strength. Normally the chain dimension is measured through scattering methods which provide the mean-square radius of gyration. The dielectric normal mode spectroscopy is a unique method for direct determination of the end-to-end distance.[2] In this study we aim to determine the parallel dipole moment of PBO for future studies of the conformation of PBO chains in solutions and in more complex systems. In regard to the relaxation strength of polyethers, it is known that the intensity of the normal mode of poly(styrene oxide)with R = C_6H_5 is very weak. This was reported by Stockmayer et al. for solutions and recently confirmed by us on the basis of more careful experiments.[27,28] Thus, the type A dipole moment of polyether depends strongly on the chemical structure of the side group R.

As mentioned above, the relationship between the global chain dynamics and segmental dynamics of a chain is an issue to be solved. Since polymers having the dipoles aligned perpendicular to the chain contour (type B dipoles) exhibit familiar segmental mode relaxation (α relaxation), we can conveniently study this issue by dielectric measurements of type AB polymers possessing both the type A and type B dipoles. The present dielectric data of PBO will complement such data. It is known that the successive occurrence of random local motions of a chain consisting of N segments results in fluctuation of the end-to-end distance.[29] When the correlation time for the local motions is τ_0, the terminal relaxation time is proportional to $\tau_0 N^2$ conforming to the Rouse theory.[9] We will discuss the relationship between the normal and segmental modes.

Experimental Section

Materials. Samples of PBO were prepared by polymerization of butylene oxide (1,2-epoxybutane) (Aldrich) in dry tetrahydrofuran with potassium hydride (Aldrich) as the initiator and 18-crown-6 (Wako Chemicals, Tokyo, Japan) as the catalyst.[30] Temperature of polymerization was changed from 0 to 50 °C to control MW. It was found that the average MW increased with decreasing temperature of polymerization. Thus, prepared PBO samples were fractionated with THF/methanol mixed solvent. Weight-average MW (M_w) and polydispersity index (M_w/M_n) were determined by a gel permeation chromatograph (GPC) equipped with a light scattering detector (Tosoh LS 8000). Sample characteristics are listed in Table 1. The polydispersity indices of some samples are relatively high. This causes an error in the MW dependence of the normal mode relaxation time and also causes the broadening of the shape of the ϵ'' curves for the normal mode. For the detailed

† Present address: Venture Business Lab., Chiba University, Inage, Chiba 263-8522, Japan.

* To whom correspondence should be addressed. E-mail: adachi@chem.sci.osaka-u.ac.jp.

10.1021/ma0516384 CCC: $30.25
Published on Web 09/30/2005

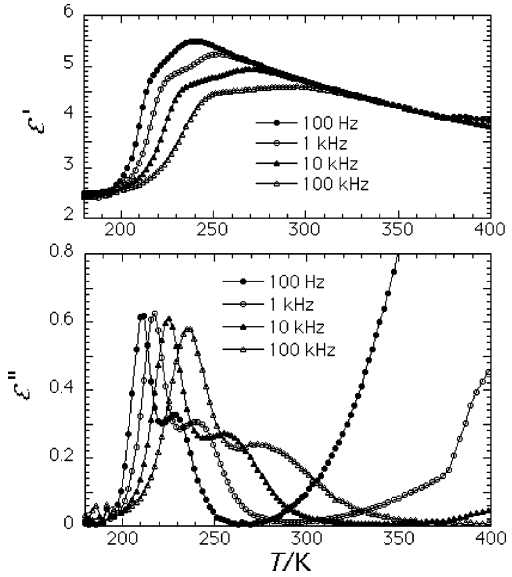

Figure 1. Temperature dependences of dielectric constant ϵ' and loss factor ϵ'' for PBO-5.

Table 1. Weight-Average Molecular Weight M_w and Polydispersity Index M_w/M_n of PBO Samples

code	$10^{-3}M_w$	M_w/M_n	code	$10^{-3}M_w$	M_w/M_n
PBO-5	4.5	1.21	PBO-36	36.0	1.15
PBO-9	8.8	1.17	PBO-37	36.8	1.58
PBO-12	12.3	1.22	PBO-45	45.0	1.20
PBO-18	18.0	1.65	PBO-50	49.9	1.31
PBO-21	20.5	1.08	PBO-59	58.8	1.31
PBO-24	23.7	1.63	PBO-85	85.0	1.28

analyses of the data, this should be taken into account. The glass transition temperature T_g was measured on representative samples of PBO-12 and PBO-50. T_gs of both samples were 199 K.

Methods. T_g was measured by a differential scanning calorimeter (Seiko Instruments & Electronics Ltd., DSC-20, Japan) at a heating rate of 10 K/min. T_g was determined as the middle point of the transition. Dielectric measurements were performed by using two RLC meters (QuadTech, models 1693 and 7600). The capacitance cell for measurements of viscous liquids was reported previously.[14] The electrodes were made of gold-plated brass and were not broking electrodes.

Results and Discussion

Temperature Dependence of Dielectric Constant and Loss. Figures 1 and 2 show the representative temperature dependence curves of the dielectric constant ϵ' and the loss factor ϵ'' for PBO with two different MW. It is seen in Figures 1 and 2 that the relatively sharp loss peaks appearing in the range from 200 to 250 K are almost independent of MW. Furthermore, the loss peak at 100 Hz is observed ca. 20 K above T_g (= 199 K) of PBO. This behavior is typical of the segmental mode (the α_s process) of amorphous polymers. On the other hand, we see that the high-temperature process shifts to high temperature with increasing molecular weight (MW). For PBO-5 the high-temperature peak appears around 230 K at 100 Hz, but in PBO-24, it appears around 270 K. This indicates that the mobility decreases with MW and hence this process can be assigned to the normal mode process (the α_n process). This behavior is more clearly seen in Figure 3 in which the ϵ'' curves at 1 kHz of PBOs with various MW are plotted. A weak loss peak can be seen around 150 K. This low-temperature peak is also independent of MW and can be assigned to the secondary relaxation process (β process).

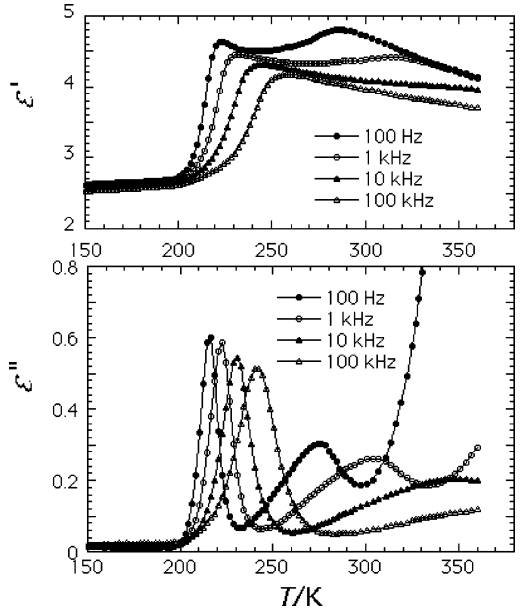

Figure 2. Temperature dependences of dielectric constant ϵ' and loss factor ϵ'' of PBO-24.

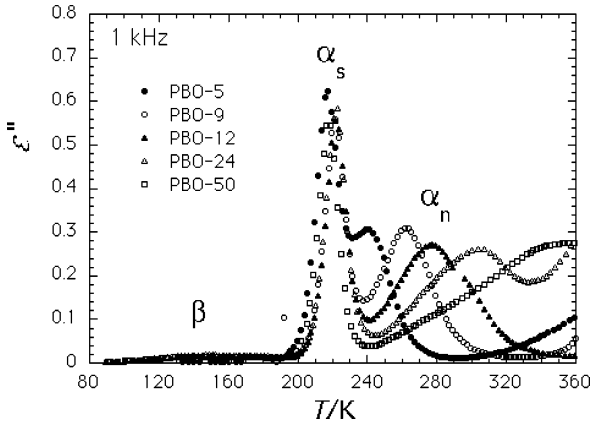

Figure 3. Temperature dependence of dielectric loss factor ϵ'' of PBO with various molecular weights.

In Figures 1 and 2, the ϵ' curves exhibit dispersions in the temperature ranges where corresponding loss peaks appear. The jump of the ϵ' curve is equal to the relaxation strength. In the temperature range above the dispersion region, ϵ' decreases monotonically due to the decrease of the relaxation strength which is proportional to the inverse of temperature. Decrease of the density with increasing temperature is also the origin of the decrease of ϵ' with temperature.

Frequency Dependence of ϵ''. Figures 4 and 5 show the representative frequency dependences of ϵ'' in the range of the α_s and α_n modes for PBO-5 and PBO-24, respectively. Comparing these curves with the corresponding temperature dependence curves of ϵ'', we assign the low- and high-frequency peaks to the normal mode and segmental mode, respectively. As observed for the other type A polymers,[1,2] the separation of the segmental and normal modes increases with increasing MW.

The separation between the normal mode and the segmental mode for PBO samples with higher MW than PBO-24 becomes wider than our experimental window. Therefore, we used time−temperature superposition

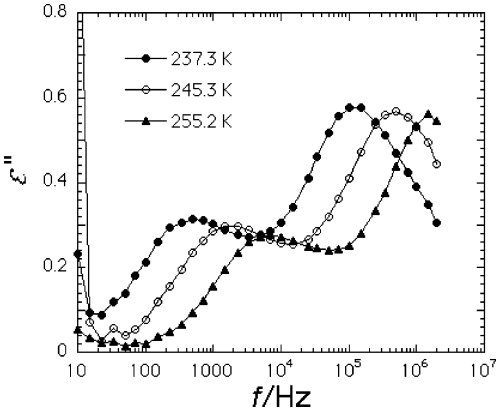

Figure 4. Frequency dependence of ϵ'' of PBO-5 in the temperature range where the segmental and normal modes are observed. Temperatures of measurements are given in the graph in K.

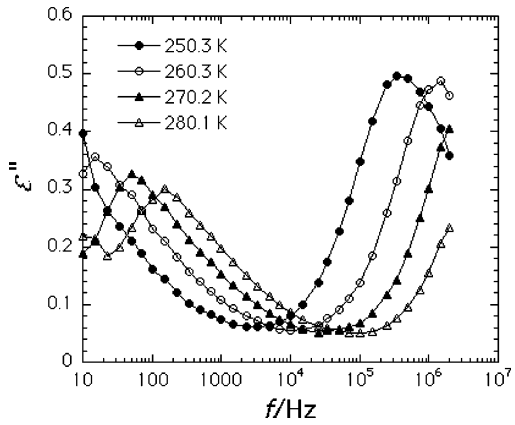

Figure 5. Frequency dependence of ϵ'' of PBO-24 in the temperature range where the segmental and normal modes are observed. Temperatures of measurements are given in the graph in K.

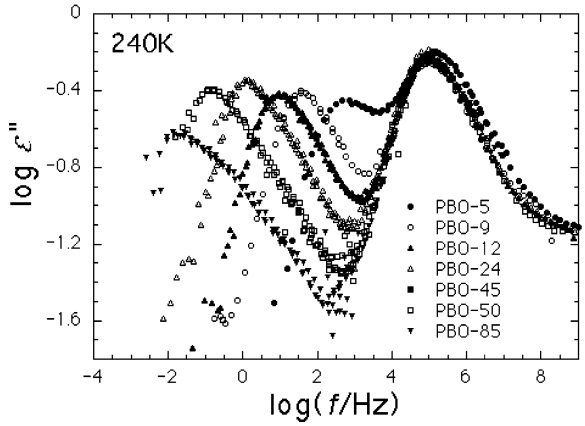

Figure 6. Master curves of ϵ'' of PBO at 240 K.

principle to observe frequency dependence of ϵ'' over a wide frequency range. Figure 6 shows the master curves of ϵ'' at 240 K for representative PBOs including the low-MW PBOs. The low-frequency peak is due to the normal mode relaxation and shifts to low-frequency side with increasing MW. The segmental mode process around log $f = 5$ is almost independent of molecular weight.

The temperature dependences of loss maximum frequencies f_m for the segmental and normal modes of PBO-5, PBO-9, and PBO-12 are compared in Figure 7 in order to examine the relationship between the

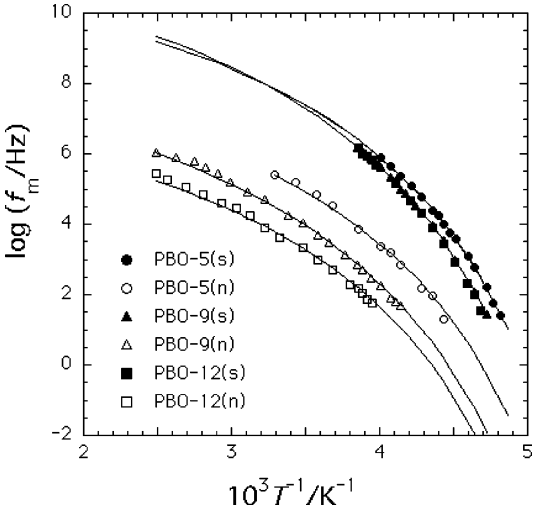

Figure 7. Arrhenius plots of the loss maximum frequencies f_m for PBO-5, PBO-9, and PBO-12. The marks (n) and (s) represent the normal and segmental modes, respectively.

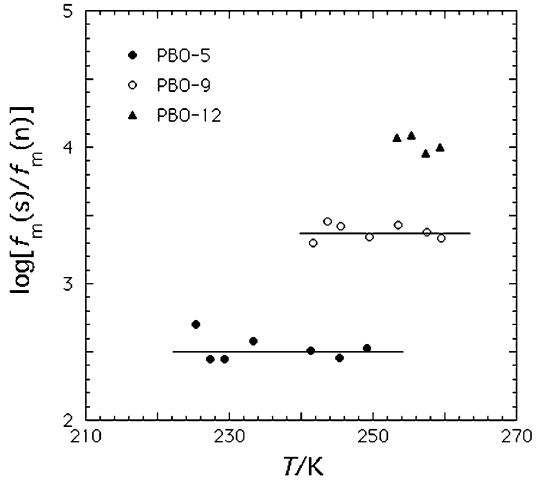

Figure 8. Temperature dependence of the separation of the normal mode and segmental mode.

relaxation times ($= {}^1/_2\pi f_m$) of the normal and segmental modes. For the segmental modes, the plots (closed keys) are almost independent of MW. For PBO-05 the relaxation frequencies are slightly higher than the others due to the effects of chain ends.

As shown in Figure 7, the temperature range in which both the normal and segmental modes can be observed at the same temperature is limited. Using those limited data, we plotted the separation of these processes log-$[f_m(s)/f_m(n)]$ in Figure 8. The separation is independent of temperature within the experimental error. This agrees with our previous report that $\log[f_m(s)/f_m(n)]$ for *cis*-polyisoprene is independent of temperature in the range $T > T_g + 30$ K.[31] In the range $T < T_g + 30$ K, $\log[f_m(s)/f_m(n)]$ decreases with decreasing temperature. Schönhals[32] reported that $\log[f_m(s)/f_m(n)]$ in *cis*-polyisoprene and PPO is almost constant in the range of temperature $T_g + 30 < T < T_g + 50$ K, and in the range above $T_g + 50$ K, it decreases slightly with increasing temperature. However, the change is less than ± 0.1 decades, and we can regard that $\log[f_m(s)/f_m(n)]$ in the range $T > T_g + 30$ K is independent of temperature within an experimental error.

It is seen in Figure 7 that the temperature dependences of $f_m(s)$ and $f_m(n)$ are of the Vogel−Fulcher type:[33,34]

$$\log f_m = A - \frac{B}{T - T_0} \quad (1)$$

where A, B, and T_0 are the constants. First, we determined these parameters for the segmental modes and listed in Table 2. The solid lines in Figure 7 indicate eq 1. If $\log[f_m(s)/f_m(n)]$ is independent of temperature, the parameters of B and T_0 for the normal and segmental modes should be the same. We tested this expectation assuming that B and T_0 for the normal mode are the same as those for segmental mode and plotted eq 1 by the solid lines. As is seen in Figure 7, the experimental data for the normal modes conform approximately to eq 1 thus drawn. This indicates that $\log[f_m(s)/f_m(n)]$ is independent of temperature in more wider range than that examined in Figure 8.

Verdier and Stockmayer performed a computer simulation to examine the relationship between the rate of local motion and the chain dynamics for a chain consisting of N beads placed on the lattice points of a cubic lattice.[29] Each bead jumps randomly to one of the neighboring lattice points. The successive occurrence of random local jumps of the beads results in fluctuation of the end-to-end distance. They found that the longest relaxation time τ_1 for the fluctuation of the end-to-end distance is proportional to N^2 conforming to the Rouse theory.[9] They also proposed theoretically the following relationship:

$$\tau_1 = K(N-1)^2\tau_0 \quad (2)$$

where K is the constant close to unity and τ_0 is the correlation time for local jump of the segments. Since $N \gg 1$, τ_1 is proportional to $N^2\tau_0$. It is reasonable to consider that the experimentally observed τ_n and τ_s correspond to τ_1 and τ_0, respectively. This equation explains well the present experimental results; i.e., although τ_0 changes rapidly with temperature, $f_m(s)/f_m(n)$ remains constant.

Two arguments may be necessary. One is the average size of segment corresponding to the bead of the Verdier–Stockmayer model. In classical models, local segmental motions occur through internal rotation of the skeletal bonds, and the several monomeric units move cooperatively as represented by the models of "crankshaft motion"[35,36] and "three-bond jump".[37,38] However, recent studies of computer simulation have revealed that those modeles are not correct.[39–42] Here we assume that the average number of the monomeric units involved in such segmental motions is n. Then N of eq 2 is given by x/n, where x is the degree of polymerization. If n changes with temperature, τ_n/τ_s depends on temperature. The experimental results indicate that the size of segmental motions does not change largely in the range of relatively higher temperature than T_g. However, in the range of $T < T_g + 30$ K, the mechanism of the segmental mode depends on temperature and n increases. Increase of the size of intermolecular cooperative motions near T_g may be the origin.

In this context, the dependence of $\log[f_m(s)/f_m(n)]$ on composition in mixed systems is an interesting issue. For concentrated solutions of *cis*-polyisoprene in toluene, we have found that $\log[f_m(s)/f_m(n)]$ decreases with decreasing concentration.[43] This indicates that with decreasing concentration hindrances for segmental motions become weak and hence segmental motions of larger size than in undiluted state can occur. Then n tends to increase with decreasing concentration.

Table 2. Parameters of the Vogel–Fulcher Equation for the Segmental Mode and the Normal Mode

	segmental mode			normal mode		
code	A	B/K	T_0/K	A	B/K	T_0/K
PBO-5	11.18	482.2	158.2	8.72	482.2	158.2
PBO-9	11.62	554.4	157.3	8.29	554.4	157.3
PBO-12	11.27	499.3	161.8	7.32	499.3	161.8

The second problem is whether the linearity of the longest relaxation time with respect to τ_0 holds even in entangled states. Equation 2 represents the proportionality of the Rouse relaxation time τ_R and local correlation time τ_0, and hence one may expect that eq 2 is applicable only to unentangled systems. However, according to the Doi–Edwards theory,[44] the longest relaxation time τ_d (tube disengagement time) is proportional to $M\tau_R(M)$, where $\tau_R(M)$ is the Rouse relaxation time in the hypothetical state where the entanglement effects are absent (see eq 9). In more sophisticated theories of modified tube theories such as constraint release[45] or contour length fluctuation,[46] τ_d is factored by a function of M, and M_e and is still proportional to $\tau_R(M)$. Therefore, we can expect that the longest relaxation time in entangled states is also proportional to τ_0.

Relaxation Strength and Dipole Moments. The relaxation strength for the segmental mode $\Delta\epsilon_s$ and that for the normal mode $\Delta\epsilon_n$ have been determined from the Cole–Cole plots and are listed in Table 2. Then the effective dipole moment for the segmental mode has been calculated with the Onsager–Kirkwood equation:[47,48]

$$\Delta\epsilon = \frac{4\pi N g p_B^2}{3k_B T}\frac{(\epsilon_U + 2)^2\epsilon_R}{3(2\epsilon_R + \epsilon_U)} \quad (3)$$

where N is the number of the monomer unit in unit volume, g the Kirkwood correlation parameter, and p_B the type B dipole moment of the monomer unit. It is noted that eq 3 is the expression in the cgs-esu unit. From the average values of $\Delta\epsilon_s$ given in Table 2, the value of $g^{1/2}p_B$ is determined to be 2.63×10^{-30} C m = 0.79 D (D: Debye unit) with the density 0.98 g/cm^3.[10] The dominant dipole moment of polyethers is the ether group, and the dipole vector is directed in the direction perpendicular to the chain contour (type B).

The relaxation strength $\Delta\epsilon_n$ for the normal mode in the electro static unit (esu) is given by[3]

$$\frac{\Delta\epsilon_n}{C} = \frac{4\pi N_A \mu^2 \langle r^2\rangle}{3k_B TM} F \quad (4)$$

where C is the concentration in the units of g/mL, μ the dipole moment per unit contour length, $\langle r^2\rangle$ the mean-square end-to-end distance, and F the internal field factor. In the present case of undiluted polymers, C is equal to the density ρ of bulk PBO. Stockmayer and Baur proposed to use the Lorentz–Lorenz equation for F.[49] Later we found that for random coil the internal field should be equal to macroscopic field and hence $F = 1$.[50] Matsushima et al.[51] measured light scattering and viscosity on dilute solution of PBO in a Θ solvent (2-propanol) at 303 K. They reported the unperturbed dimension $(\langle r^2\rangle/M)^{1/2}$ to be 0.700×10^{-8} (cm mol$^{1/2}$ g$^{-1/2}$). From this value and the relaxation strength $\Delta\epsilon_n$, μ is determined to be 1.65×10^{-11} esu (5.50×10^{-21} C). Previously, we determined $\Delta\epsilon_n$ of poly(propyrene oxide)

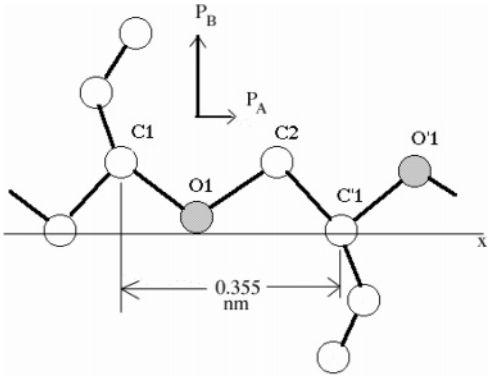

Figure 9. Structure of PBO and the type A and B dipoles.

Table 3. Relaxed Dielectric Constant ϵ_R, Unrelaxed Dielectric Constant ϵ_U, and Relaxation Strength $\Delta\epsilon_s$ for the Segmental Mode and $\Delta\epsilon_n$ for the Normal Mode

	segmental mode				normal mode			
code	T/K	ϵ_R	ϵ_U	$\Delta\epsilon_s$	T/K	ϵ_R	ϵ_U	$\Delta\epsilon_n$
PBO-12	221.6	4.53	2.58	1.95	319.7	4.51	3.76	0.75
PBO-24	220.5	4.68	2.75	1.93	319.1	4.51	3.78	0.73
PBO-45	220.5	4.60	2.65	1.95	319.5	4.34	3.59	0.75

(PPO) to be 0.52 at 236 K and μ of 1.10×10^{-11} esu with $F = 1$.[8] In contrast those data, we recently reported that the relaxation strength for the normal mode of poly(styrene oxide) (PSO, R = C_6H_5) is zero within experimental error.[28] Comparing μ of PBO, PPO, and PSO, we see that the side group R of polyethers affects strongly the parallel component of the dipole moment.

Now we determine the type A and type B components of the dipole moment per monomeric unit. Figure 9 shows the structure of the PBO molecule stretched fully in the direction along x axis (all trans conformation). The length of the monomer unit becomes 0.355 nm as indicated in the figure. Here the C−C and C−O bond lengths are assumed to be 0.153 and 0.142 nm, respectively, and the C−C−O and C−O−C angles to be 109° and 110°, respectively. Thus, the type A component p_A becomes 0.59 D (= μ times 0.355 nm). Since the bond moment of C2−C′1 is almost zero, p_A locates on the C1−O−C2 group, as shown in Figure 9. To determine the direction of p_A, we calculated the local charges of the atoms of the PBO chain with the method of molecular dynamics (AM1). Results indicate that the positive charges of C2 including two attached H atoms is higher than that of the sum of charges of C1 including one attached H atom. Thus, p_A is directed as indicated by the arrow in Figure 9.

The dipole moment of the ether group is reported to be 1.2 D for various low molecular weight ethers.[52] Therefore, the type B component (p_B) is calculated to be 1.04 D. Since $g^{1/2}p_B$ is determined to be 0.79 D, g of PBO becomes 0.87, indicating that the dipoles of the ether groups tend to orient antiparallel.

Molecular Weight Dependence of Normal Mode Relaxation. In this section the MW dependence of the relaxation time for the normal mode τ_n is discussed. Before plotting τ_n against M, it is needed to correct the M dependence of the friction coefficient. For high molecular weight polymers, τ_n can be written by a form

$$\tau = \zeta(T)F(M) \tag{5}$$

where $\zeta(T)$ and $F(M)$ are the friction factor and the structure factor, respectively. The friction factor is a function of temperature and is independent of the architecture of the polymer molecule. However, it is known that $\zeta(T)$ depends weakly on M for low molecular weight polymers. Therefore, it is required to reduce the data of low MW samples into an isofriction state. Comparing eq 2 and eq 5, we note that $\zeta(T)$ is proportional to the rate of local motion τ_0. Therefore, we converted τ_n of PBO-5 and those reported in ref 10 into the values ($\tau_{n\zeta}$) at the isofriction state of the high molecular weight samples using the data of τ_s. For the other high-MW samples this correction was not necessary.

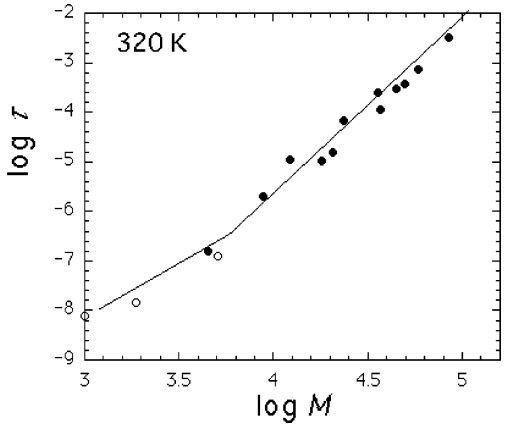

Figure 10. Molecular weight dependence of the relaxation time $\tau_{n\zeta}$ for the normal mode. The open circles indicate the data reported in ref 10.

The relaxation times $\tau_{n\zeta}$ for the normal mode are plotted against MW in Figure 10 together with the data of ref 10. It is seen that the plots exhibit a break at the characteristic molecular weight M_c of about 6000 ± 2000. Unfortunately, the data points are rather scattered, resulting in a relatively large error of M_c. The present value of M_c should be confirmed by measurements of the plateau modulus from which the molecular weight between entanglements $M_e \approx M_c/2$ can be determined. The slope of the plots in the range of MW less than M_c is 2.0, and in $M > M_c$ the slope is 3.4 ± 0.1.

Here we summarize briefly the theories of the normal mode relaxation. The Rouse theory predicts that the complex dielectric constant ϵ^* for the normal mode of nonentangled chains is given by[9]

$$\epsilon^* - \epsilon_U = \frac{8\Delta\epsilon_n}{\pi^2} \sum_{p=\text{odd}}^{N} \frac{1}{p^2(1 + i\omega\tau_p)} \tag{6}$$

where $\Delta\epsilon_n$ is the relaxation strength and is given by eq 4, τ_p the relaxation time for the pth mode, and ω the angular frequency. τ_p is given by

$$\tau_p = \frac{\zeta N_b^2 b^2}{3\pi^2 k_B T p^2} \tag{7}$$

where ζ is the friction for one bead, N_b the number of beads per chain, b the average distance between neighboring beads, and k_BT the thermal energy. The longest relaxation time τ_1 of undiluted polymers is expressed by using the zero shear viscosity η_0:

$$\tau_1 = \tau_R = \frac{12\eta_0 M}{\pi^2 \rho RT} \tag{8}$$

where ρ is the density.

For entangled chains with M above M_c, tube models may be applied.[44] According to the original tube model, the relaxation spectrum is represented by eq 6, and the longest relaxation time τ_d in the entangled chains is given by

$$\tau_d = \frac{3\tau_R(M_e)M^3}{{M_e}^3} = \frac{3\tau_R(M)M}{M_e} \quad (9)$$

where τ_R is the longest relaxation time of the Rouse theory and M_e the molecular weight between entanglement. The theory predicts that τ_d is proportional to $M^{3.0}$.

Returning to the experimental results given in Figure 10, we note that the exponent 3.4 for the MW dependence of τ_n is higher than the theoretical prediction. The discrepancy between the theory and the experiment can be ascribed to the constraint release mechanism proposed by Graessley;[45] i.e., the tube itself fluctuates since the surrounding chains also move at the same rate as the reference chain. If the reference chain is put in a matrix of high molecular weight, the chain dynamics conforms to the theory. This was confirmed experimentally for dilute blends of *cis*-polyisoprene with high-MW *cis*-PI and those of PI in polybutadiene.[19] The exponent of ca. 3.5−3.7 in monodisperse PI was explained by the constraint release model. It is expected that the chain dynamics of PBO is similar to that of PI.

Conclusion

We have reported the results of dielectric measurements on undiluted poly(butylene oxide) (PBO) in the frequency range from 0.01 to 1000 kHz. PBO exhibits the dielectric normal mode relaxation (the α_n process) due to fluctuation of the end-to-end vector and the segmental relaxation (the α_s process) due to local motions in the temperature range from 200 to 360 K. The α_n process depends strongly on molecular weight (MW), but the α_s process does not. The relaxation time τ_n for the normal mode and τ_s for the segmental mode conform to the Vogel−Fulcher equation, and the ratio of τ_n/τ_s does not depend on temperature in the range of temperature above $T_g + 25$ K where the glass transition temperature T_g is 199 K. This behavior can be explained on the basis of the Verdier−Stockmayer model which predicrs $\tau_n = KN^2\tau_s$, where K is the constant and N the number of the segments per chain. The dipole moment per unit contour length of the PBO chains becomes 1.65×10^{-11} esu (5.50×10^{-21} C) from the relaxation strength for the normal mode. The type A component p_A per monomer unit has been also determined to be 0.59 D (D: Debye unit). From the relaxation strength for the segmental mode, $g^{1/2}p_B$ is determined to be 0.79 D and $g = 0.87$, where g is the Kirkwood correlation factor. Therefore, the type B component (p_B) is calculated to be 1.04 D. The MW dependence of τ_n changes around the characteristic molecular weight M_c (=6000); i.e., in the range of $M < M_c$ τ_n is proportional to M,$^{2.0}$, and in the range $M > M_c$ τ_n is proportional to $M^{3.4}$.

References and Notes

(1) Stockmayer, W. H. *Pure Appl. Chem.* **1967**, *15*, 539.
(2) Adachi, K.; Kotaka, T. *Prog. Polym. Sci.* **1993**, *16*, 585.
(3) Adachi, K. Dielectric Relaxation in Polymer Solutions In *Dielectric Spectroscopy of Polymeric Materials*; Runt, J. P., Fitzgerald, J. J., Eds.; American Chemical Society: Washington, DC, 1997; Chapter 9, pp 261−282.
(4) Baur, M. E.; Stockmayer, W. H. *J. Chem. Phys.* **1965**, *43*, 4319.
(5) Burke, J. J.; Stockmayer, W. H. *Macromolecules* **1969**, *3*, 647.
(6) Schlosser, E.; Schonhals, A. *Prog. Colloid Polym. Sci.* **1993**, *91*, 158.
(7) Schonhals, A.; Kremer, F. *J. Non-Cryst. Solids* **1994**, *172−174*, 336.
(8) Hayakawa, T.; Adachi, K. *Polymer* **2001**, *42*, 1725.
(9) Rouse, P. E. *J. Chem. Phys.* **1953**, *21*, 1272.
(10) Kyritsis, A.; Pissis, P.; Mai, S.-M.; Booth, C. *Macromolecules* **2000**, *33*, 4581.
(11) Fragiadakis, D.; Bouga, M.; Kyritsis, A.; Pissis, P.; Viras, K.; Mingvanish, W. S. M.; Booth, C. *Macromol. Symp.* **2003**, *191*, 21.
(12) Adachi, K.; Kotaka, T. *Macromolecules* **1984**, *17*, 120.
(13) Adachi, K.; Kotoka, T. *Macromelecules* **1985**, *18*, 466.
(14) Imanishi, Y.; Adachi, K.; Kotaka, T. *J. Chem. Phys.* **1988**, *89*, 7585.
(15) Bose, D.; Kremer, F. *Macromelecules* **1990**, *23*, 829.
(16) Schönhals, A. *Macromolecules* **1993**, *26*, 1309.
(17) Ren, J.; Urakawa, O.; Adachi, K. *Macromolecules* **2003**, *36*, 210.
(18) Adachi, K.; Hirano, H.; Freire, J. J. *Polymer* **1999**, *40*, 2271.
(19) Adachi, K.; Wada, T.; Kawamoto, T.; Kotaka, T. *Macromolecules* **1995**, *28*, 3588.
(20) Urakawa, O.; Adachi, K.; Kotaka, T. *Macromolecules* **1993**, *26*, 2036, 2042.
(21) Serghei, A.; Kremer, F. *Phys. Rev. Lett.* **2003**, *91*, 165702.
(22) Algeria, A.; Colmenero, J.; Ngai, K. L.; Roland, C. M. *Macromolecules* **1994**, *27*, 4486.
(23) Roland, C. M.; Bero, C. A. *Macromolecules* **1996**, *29*, 7521.
(24) Watanabe, H.; Matsumiya, Y.; Inoue, T. *Macromolecules* **2002**, *35*, 2339.
(25) Floudas, G.; Reisinger, T. *J. Chem. Phys.* **1999**, *111*, 520.
(26) Petychakis, L.; Floudas, G.; Fleisher, G. *Europhys. Lett.* **1997**, *40*, 685.
(27) Matsuo, K.; Stockmayer, W. H.; Mashimo, S. *Macromolecules* **1982**, *15*, 606.
(28) Hirose, Y.; Adachi, K. *Polymer* **2005**, *46*, 1913.
(29) Verdier, R. H.; Stockmayer, W. H. *J. Chem. Phys.* **1962**, *36*, 227.
(30) Stolarzewich, A.; Neugebauer, D. *Macromol. Chem. Phys.* **1999**, *200*, 2467.
(31) Adachi, K.; Hirano, H. *Macromolecules* **1998**, *31*, 3958.
(32) Schönhals, A. Dielectric Properties of Amorphous Polymers In *Dielectric Spectroscopy of Polymeric Materials*; Runt, J. P., Fitzgerald, J. J., Eds.; American Chemical Society: Washington, DC, 1997; Chapter 3, pp 81−106.
(33) Vogel, H. *Phys. Z.* **1921**, *22*, 645.
(34) Fulcher, J. G. *J. Am. Ceram. Soc.* **1925**, *8*, 339.
(35) Shatzki, T. F. *J. Polym. Sci.* **1962**, *57*, 496.
(36) Helfand, E. *J. Chem. Phys.* **1971**, *54*, 4651.
(37) Boyer, R. F. *Rubber Rev.* **1963**, *34*, 1303.
(38) Valeur, B.; Jarry, J. P.; Geny, F.; Monnerie, L. *J. Polym. Sci., Polym. Phys. Ed.* **1975**, *13*, 667.
(39) Moe, N. E.; Ediger, M. D. *Macromolecules* **1995**, *28*, 2329.
(40) Paul, W.; Smith, G. D. *Rep. Prog. Phys.* **2004**, *67*, 1117.
(41) Bahar, I.; Cho, J. H.; Doruker, P.; Erman, B.; Haliloglu, T.; Kim, E. G.; Mattice, W. L.; Monnerie, L.; Rapold, R. F. *Trends Polym. Sci.* **1997**, *5*, 155.
(42) Baschnagel, J.; Binder, K.; Doruker, P.; Gusev, A. A.; Hahn, O.; Kremer, K.; Mattice, W. L.; Muller-Plathe, F.; Murat, M.; Paul, W.; Santos, S.; Suter, U. W.; Tries, V. *Adv. Polym. Sci.* **2000**, *152*, 41.
(43) Adachi, K.; Imanishi, Y.; Kotaka, T. *J. Chem. Soc., Faraday Trans. 1* **1989**, *85*, 1083.
(44) Doi, M.; Edwards, S. F. *J. Chem. Soc., Faraday Trans. 2* **1978**, *74*, 1789, 1802, 1818.
(45) Graessley, W. W. *Adv. Polym. Sci.* **1982**, *47*, 68.
(46) Doi, M. *J. Polym. Sci., Polym. Phys. Ed.* **1983**, *21*, 667.
(47) Onsager, L. *J. Am. Chem. Soc.* **1936**, *58*, 1486.
(48) Kirkwood, J. G. *J. Chem. Phys.* **1939**, *7*, 911.
(49) Stockmayer, W. H.; Baur, M. E. *J. Am. Chem. Soc.* **1964**, *86*, 3485.
(50) Adachi, K.; Okazaki, H.; Kotaka, T. *Macromolecules* **1985**, *18*, 1486.
(51) Matsushima, M.; Fukatsu, M.; Kurata, M. *Bull. Chem. Soc. Jpn.* **1968**, *41*, 2570.
(52) Smith, C. P. *Dielectric Behavior and Structure*; McGraw-Hill: New York, 1955; pp 297−299.

MA0516384